Indian J Phys
https://doi.org/10.1007/s12648-025-03731-9

ORIGINAL PAPER

Anisotropic core-envelope compact star model with conformal symmetry

Y K Kowa[1], J W Jape[1,3], J M Sunzu[1]* and S D Maharaj[2]

[1]Department of Mathematics and Statistics, University of Dodoma, Dodoma 338, Tanzania

[2]Astrophysics Research Centre, School of Mathematics, Statistics and Computer Science, University of KwaZulu-Natal, Durban 4000, South Africa

[3]Department of Mathematics and Statistics, Mbeya University of Science and Technology, Mbeya, Tanzania

Received: 26 February 2025 / Accepted: 09 July 2025

Abstract: In this paper, the combination of the conformal Killing vector and equations of state for double layered stars provides new solutions to the Einstein field equations in the core-envelope setting. The matter composition in the core layer obeys a linear equation of state, while in the envelope is described by a quadratic equation of state. The behavior of the matter variables in the stellar sphere is found to be well behaved, and the model satisfies stability conditions. The generated compact star model satisfies the energy and equilibrium conditions for the behavior of the natural forces. The mass, compactness, and surface redshift also fall within the required range for observed stars. Radii and masses of the stars PSRJ1903+0327, SAXJ1808.4-3658, VelaX-1, 4U1608-52, HerX-1, SMCX-1 and EXO1785-248 have been regained. This signifies the astrophysical importance of our generated class of exact solutions.

Keywords: Conformal killing vector; Einstein field equations; Compact star model; Core-envelope setting; Exact solutions

1. Introduction

Stars are formed in gas and dust clouds with a nonuniform matter distribution scattered throughout most galaxies. In astrophysics, the term compact object usually refers collectively to white dwarfs and neutron stars that form at the end of their stellar evolution [1, 2]. Compact objects have high densities and strong gravitational fields. Albert Einstein established the general theory of relativity (GR) in 1915 to study strong gravitational fields. The theory is considered to be the basic platform for investigations in stellar astrophysics. The GR theory generalizes special relativity and extends Newton's law of universal gravitation, making a combined description of gravity as a geometric property of space and time. The study of the behavior and properties of compact objects draws the attention of many researchers in astrophysics and astronomy. The Einstein field equations (EFEs) are useful in studying and understanding the structure and behavior of stellar objects. The first known solution to the EFEs was generated by Schwarzschild in 1916. Since then, several researchers have investigated these equations using different approaches and several astrophysical models have been established to provide detailed explanation for the matter distribution within stellar bodies. Currently, some solutions to the EFEs for compact star models have been generated by [3–12].

In studying compact stars, pressure anisotropy plays a vital role to describe the gravitational behavior of these objects. Anisotropy defines the difference between radial and tangential pressures. The pressure anisotropy originates due to various reasons such as the presence of solid core, phase transitions, slow rotation, viscosity-induced anisotropy, presence of type 3A super-fluid, pion condensation, and different types of fluid mixture as has been discussed in [13–15]. The presence of anisotropic pressure within relativistic fluid spheres influences stability, variations of magnetic field intensity, structure and properties such as mass, compactness factor, and maximum surface redshift due to tension within these objects as reported in

*Corresponding author, E-mail: jefta@aims.ac.za

Published online: 06 August 2025

[13, 16–24]. Recent compact star models with varying pressures include those generated by [25–29].

Equations of state (EOS) have been fruitful tools in studying behavior and properties of relativistic fluid spheres. EOS describe the material compositions within compact stars. They provide the relationship between the energy density and radial pressure of fluid spheres. Several relativistic models with equations of state have been generated in the literature. Thirukkanesh and Maharaj [30], and Babichev et al. [31] generated models for relativistic stellar bodies using a linear equation of state. Suleiman et al. [9] developed stellar models with a polytropic equation of state. Bhar et al. [32], and Estevez-Delgado et al. [33] developed compact star models in which the interior matter distribution obeys a Chaplygin equation of state. Thirukkanesh and Ragel [34], Malaver [35, 36] and Malaver and Kasmaei [37] generated relativistic models with a Van der Waals equation of state to describe the behavior of anisotropic matter distribution. Sunzu and Thomas [17], and Sunzu and Mathias [38] developed compact star models with a quadratic equation of state for the matter configurations in the presence of anisotropy.

There are good number of papers on core-envelope setting with different approaches. Models with only equations of state in core-envelope layers have been analyzed by several authors. Sunzu and Lighuda [39] constructed a double layered model with a polytropic and a quadratic equations of state. Mardan et al. [40] developed a core-envelope model for compact stars with a polytropic core and a linear envelope. Pant et al. [41] presented a study on a core-envelope model in which the core obeys a linear equation of state while the envelope obeys a quadratic equation of state. Mafa Takisa et al. [42] established a compact relativistic star model with a quadratic envelope and a quark core. Mafa Takisa and Maharaj [5] studied a double layered model using quadratic and linear equations of state in the core and envelope respectively. Nasheeha et al. [29] developed a core-envelope model for a polytropic star with distinct polytropic indexes.

Higher gravity theories have been useful in generating compact star models with physical significance. Jasim et al. [43] generated the anisotropic solution of compact objects in the frame work of $f(R, T)$ gravity theory. The solution is obtained by imposing the vanishing complexity factor condition. Maurya and Nag [44] investigated two gravitationally decoupled anisotropic solutions by imposing the condition of two systems with the same complexity factor as well as systems with zero complexity factor. Maurya et al. [45] studied the possibility of existence of anisotropic spherically symmetric solutions in the arena of modified $f(G, T)$ gravity theory. In this case, one of the metric potentials was specified to obtain the second through quasi-local mass function $e^{-\lambda} = 1 - \frac{2m}{r}$ relationship. Compact star models in core-envelope setting with Karmarkar condition have been investigated by some researchers. Mathias et al. [25] employed the Karmarkar condition to investigate the properties of double layered anisotropic stars with core described by quark linear equation of state while the envelope obeying Chaplygin gas equation of state. Mathias et al. [46] generated a neutral core-envelope stellar model admitting Karmarkar condition with the core layer satisfying a linear equation of state while quadratic equation of state employed for envelope. Ditta et al. [47], and Singh et al. [48] presented a detailed comparative analysis of embedding class one (Karmarkar condition), conformally flat, vanishing complexity factor, and conformally symmetric solutions, highlighting their effectiveness in generating new solutions to the field equations. Each of these approaches reduces the complexity of solving field equations by specifying one of the potentials to obtain the matter variables.

The use of conformal symmetry has been useful as well in studying the behavior and properties of compact stars. The imposition of conformal Killing vector (CKV) on the spacetime manifold provides specific restrictions on these potentials which in turn simplify the process of solving the field equations. There are several models generated through this approach, including [49–52]. Single layered stars admitting conformal symmetry and equations of state were investigated by some few authors in the past. Jape et al. [53] generated a relativistic compact star model admitting conformal Killing vector and a linear equation of state in the presence of charge. Christopher et al. [54] analyzed the properties of a relativistic charged compact star by employing both the conformal Killing vector and a quadratic equation of state. It is evident that studies on multi-layered stars that combine the conformal symmetry and equations of state are lacking in the existing literature. We are interested in studying the behavior and properties of a neutral anisotropic core-envelope star through merging both the CKV and equations of state. We describe the inner layer with a linear equation of state while the envelope obeys a quadratic equation of state.

To achieve the objectives of this work, the paper is organized as follows: Sect. 2 introduces the basic field equations of the study while the conformal symmetry is described in Sect. 3. The transformation of variables is done in Sect. 4. In Sect. 5, the metric potential is specified to determine the core-envelope matter variables. The junction conditions are discussed in Sect. 6. The model validation through different conditions is found in Sect. 7 while a detailed discussion is given in Sect. 8.

2. Basic field equations

We consider the gravitational line element in Schwarzschild coordinates for a static spherically symmetric fluid distributions defined as

$$ds^2 = -e^{2\nu(r)}dt^2 + e^{2\lambda(r)}dr^2 + r^2(d\theta^2 + \sin^2\theta d\phi^2), \tag{1}$$

where $\nu(r)$ and $\lambda(r)$ are gravitational metric potentials which are functions of the radial coordinate r.

The exterior spacetime line element is given by

$$ds^2 = -\left(1 - \frac{2M}{r}\right)dt^2 + \left(1 - \frac{2M}{r}\right)^{-1}dr^2 + r^2(d\theta^2 + \sin^2\theta d\phi^2), \tag{2}$$

where the variable M defines the mass of the core-envelope star. The energy momentum tensor for the uncharged anisotropic sphere is given by

$$T_{ij} = \text{ diag }(-\rho,\ p_r,\ p_t,\ p_t), \tag{3}$$

with the quantities ρ, p_r, and p_t represent the energy density, radial pressure and tangential pressure, respectively. By assuming the coupling constant $\frac{8\pi G}{c^4} = 1$, the field equations for the uncharged anisotropic core-envelope star become

$$\frac{1}{r^2}\left(1 - e^{-2\lambda} + \frac{2\lambda'}{r}e^{-2\lambda}\right) = \rho, \tag{4a}$$

$$-\frac{1}{r^2}\left(1 - e^{-2\lambda} + \frac{2\nu'}{r}e^{-2\lambda}\right) = p_r, \tag{4b}$$

$$e^{-2\lambda}\left(\nu'' + \nu'^2 - \nu'\lambda' + \frac{\nu'}{r} - \frac{\lambda'}{r}\right) = p_t, \tag{4c}$$

$$p_t - p_r = \Delta, \tag{4d}$$

where the primes ($'$) indicate derivatives with respect to radial distance r, and Δ is the anisotropic pressure for the stellar fluid. The mass of the core-envelope star is given as

$$M(r) = \frac{1}{2}\int_0^r \varphi^2\rho(\varphi)d\varphi. \tag{5}$$

3. Conformal symmetry

We consider the spacetime manifold admitting conformal symmetry. The imposition of the conformal Killing vector helps to simplify the EFEs in the system (4). Together with the equation of state, the use of CKV leads to new exact solutions for the core-envelope model. The conformal Killing vector is defined as

$$L_X g_{ab} = 2\eta g_{ab}, \tag{6}$$

where g_{ab} is the metric tensor, η is the conformal factor, L_X is the Lie derivative operator, and $\mathbf{X}$ is the vector field. In generating the core-envelope model, it is assumed that both the vector field $\mathbf{X}$ and the conformal factor η are non-static. Using this assumption, the conformal Killing equation (6) is expressed as

$$\mathbf{X} = \alpha(t,r)\frac{\partial}{\partial t} + \beta(t,r)\frac{\partial}{\partial r}, \tag{7a}$$

$$\eta = \eta(t,r). \tag{7b}$$

To solve Eq. (6), we consider the associated Weyl tensor integrability condition given by

$$L_X C^a_{bcd} = 0, \tag{8}$$

where C^a_{bcd} are the Weyl tensor components. Now, using Eq. (8) together with system (7), the conformal Killing equation (6) simplifies to a nonlinear differential equation

$$\nu'' + (\nu')^2 - \nu'\lambda' - \frac{\nu' - \lambda'}{r} + \frac{1}{r^2} = \frac{e^{2\lambda}(1+j)}{r^2}, \tag{9}$$

where j is a constant. This is a nonlinear equation but it does admit a general solution. It has been integrated as indicated in Maharaj et al. [55] and Herrera et al. [56], and its solution is given by

$$e^{\nu} = \begin{cases} Ar\exp\left(\sqrt{1+j}\int\frac{e^{\lambda}}{r}dr\right) + Br\exp\left(-\sqrt{1+j}\int\frac{e^{\lambda}}{r}dr\right), & 1+j>0 \\ Ar\int\frac{e^{\lambda}}{r}dr + Br, & 1+j=0 \\ Ar\exp\left(\sqrt{-(1+j)}\int\frac{e^{\lambda}}{r}dr\right) + Br\exp\left(-\sqrt{-(1+j)}\int\frac{e^{\lambda}}{r}dr\right), & 1+j<0 \end{cases} \tag{10}$$

where A and B are constant parameters. The case $j = 0$ indicates that the spacetime manifold is conformally flat, otherwise $j \neq 0$.

4. Transformation of matter variables

We adopt the transformation proposed by Durgapal and Bannerji [57] to simplify the field equations (4). This transformation is given by

$$x = Cr^2, \quad z(x) = e^{-2\lambda(r)}, \quad y^2(x) = e^{2\nu(r)}. \tag{11}$$

By these transformations, the Einstein field equations (4) are transformed to

$$\frac{1-z}{x} - 2\dot{z} = \frac{\rho}{C}, \tag{12a}$$

$$4z\frac{\dot{y}}{y} + \frac{z-1}{x} = \frac{p_r}{C}, \tag{12b}$$

$$4xz\frac{\ddot{y}}{y} + (4z + 2x\dot{z})\frac{\dot{y}}{y} + \dot{z} = \frac{p_t}{C}, \tag{12c}$$

$$\frac{1-z}{x} + 4xz\frac{\ddot{y}}{y} + 2x\dot{z}\frac{\dot{y}}{y} + \dot{z} = \frac{\Delta}{C}. \tag{12d}$$

The dots $(\cdot)$ in the system (12) stand for the derivative of the variables with respect to the radial coordinate x.

5. New exact solution

To tract the new exact solution for the core-envelope compact star model, we transform condition (10) into a new relation in the gravitational potentials y and z. This is done by using the transformation (11) with $j = 2(n-1)$. This process gives

$$y = \begin{cases} A\sqrt{x}\exp\left(\frac{1}{2}\sqrt{2n-1}\int\frac{dx}{x\sqrt{z}}\right) \\ +B\sqrt{x}\exp\left(\frac{-1}{2}\sqrt{2n-1}\int\frac{dx}{x\sqrt{z}}\right), & n > \frac{1}{2} \\ \frac{A}{2}\sqrt{x}\int\frac{dx}{x\sqrt{z}} + B\sqrt{x}, & n = \frac{1}{2} \\ A\sqrt{x}\exp\left(\frac{1}{2}\sqrt{-(2n-1)}\int\frac{dx}{x\sqrt{z}}\right) \\ +B\sqrt{x}\exp\left(\frac{-1}{2}\sqrt{-(2n-1)}\int\frac{dx}{x\sqrt{z}}\right), & n < \frac{1}{2} \end{cases} \tag{13}$$

If we specify the gravitational potential z on physical grounds, we can obtain the second gravitational potential y through integration of (13).

5.1. Metric potentials

On a physical basis, we specify the ansatz for z so that we can obtain the second metric potential y from Eq. (13). This specification is done so that a well behaved core-envelope model with CKV is generated. The ansatz for z is specified as

$$z(x) = \frac{1}{(ax-1)^2}, \tag{14}$$

where $ax \neq 1$. It is evident from Eq. (14) that when $x = 0$, the potential $z = 1$. This is necessary condition when generating stellar models which are free from physical and geometric singularities. Similar forms to gravitational potential (14) have been adopted by several authors to generate physically acceptable relativistic models. Thirukkanesh and Ragel [34] studied the behavior of relativistic compact objects by using the Van der Waals equation of state where two classes of exact solutions were obtained. Jape et al. [28] investigated properties of single layered stars by combining the conformal Killing vector and a linear equation of state. Christopher et al. [54] used a similar form to study the characteristics of a charged anisotropic star in a single layered setting by combination of conformal Killing vector and quadratic equation of state. Notably, the metric (14) is just like the Tolman metric ansatz $z = \frac{1}{1 + Ar^2 + Br^4}$. If we assume $A = -2a$ and $B = a^2$, then we get the similar metric function [58–60]. In this study, the metric function (14) is used to study the behavior and properties of a multi-layered star that admits conformal symmetry with distinct equations of state for the core and envelope layers. We use the same choice for a core-envelope model with CKV which is missing in other treatments. Using Eq. (14) into (13), with $n = 1$, we find the gravitational potential y as

$$y = A\exp\left(\frac{ax}{2}\right) + Bx\exp\left(\frac{-ax}{2}\right). \tag{15}$$

5.2. The core-envelope model

The radial distance corresponding to core and envelope are denoted by R_{co} and R_{ev} respectively. The metric potentials and their derivatives were substituted into system (12) for computation of ρ, p_r, p_t, and $\triangle$ for the core and envelope layers, respectively.

5.2.1. The core layer

The radius R_{co} of the inner region of a star is given as $0 \le r \le R_{co}$, with its corresponding line element given by

$$ds^2|_{co} = -e^{2\nu_{co}(r)}dt^2 + e^{2\lambda_{co}(r)}dr^2 + r^2(d\theta^2 + \sin^2\theta d\phi^2). \tag{16}$$

The core is considered to compose of harder material obeying a linear equation of state defined as

$$p_{rco} = \gamma\rho_{co} - \kappa, \tag{17}$$

where γ and κ are real constants such that $\gamma \neq 0$.

Using Eqs. (14), (15), and (17) in system (12), the matter variables for the core layer of the star become

$$\rho_{co} = \frac{C\,a\,(a^2 x^2 - 3\,a\,x + 6)}{(a\,x - 1)^3}, \tag{18a}$$

$$p_{rco} = \frac{C\,\gamma a\,(a^2 x^2 - 3\,a\,x + 6)}{(a\,x - 1)^3} - \kappa, \tag{18b}$$

$$\triangle_{co} = \frac{2\,C\,a^2\,x\,(a\,x - 3)}{(a\,x - 1)^3}, \tag{18c}$$

$$p_{tco} = \frac{2\,C\,a^2\,x\,(a\,x - 3)}{(a\,x - 1)^3} + \frac{C\,\gamma a\,(a^2 x^2 - 3\,a\,x + 6)}{(a\,x - 1)^3} - \kappa. \tag{18d}$$

5.2.2. *The envelope layer*

For the outer surface, the radial distance becomes $R_{co} < r \le R_{ev}$, and its corresponding line element is written as

$$ds^2|_{ev} = -e^{2\nu_{ev}(r)}dt^2 + e^{2\lambda_{ev}(r)}dr^2 + r^2(d\theta^2 + \sin^2\theta d\phi^2). \tag{19}$$

The outer layer of the star is considered to contain neutron fluid which is described by a quadratic equation of state of the form

$$p_{rev} = \xi\rho_{ev}^2 - \Pi, \tag{20}$$

where ξ and Π are real constants such that $\xi \neq 0$.

Using Eqs. (14), (15) and (20), the system of field equations (12) for the envelope becomes

$$\rho_{ev} = \frac{Ca(a^2x^2 - 3ax + 6)}{(ax - 1)^3}, \tag{21a}$$

$$p_{rev} = \frac{\xi C^2 a^2 (a^2x^2 - 3ax + 6)^2}{(ax - 1)^6} - \Pi, \tag{21b}$$

$$\triangle_{ev} = \frac{2aC(ax - 2)}{(ax - 1)^2}), \tag{21c}$$

$$p_{tev} = \frac{2aC(ax - 2)}{(ax - 1)^2} + \frac{\xi C^2 a^2 (a^2x^2 - 3ax + 6)^2}{(ax - 1)^6} - \Pi. \tag{21d}$$

Through transformations (11), and using Eq. (21a), the mass function (5) reduces to

$$M = \frac{C^2\,a\,x\,\sqrt{\frac{x}{C}}\,(a\,x - 2)}{(a\,x - 1)^2}. \tag{22}$$

The mass function (22) is important to describe the behavior of the surface redshift and the compactness factor.

6. Junction conditions

6.1. Junction conditions at the core-envelope interface

Taking into account the junction criterion for the radial pressure, and gravitational potentials to be continuous at the interface of core and envelope, the junction conditions at the core-envelope are given as

$$e^{2\lambda_{co}}(R_{co}) = e^{2\lambda_{ev}}(R_{ev}), \tag{23a}$$

$$e^{2\nu_{co}}(R_{co}) = e^{2\nu_{ev}}(R_{ev}), \tag{23b}$$

$$p_{rco}(R_{co}) = p_{rev}(R_{ev}). \tag{23c}$$

6.2. Junction conditions at the boundary

The junction condition of the envelope at the boundary ($r = R_{ev}$) requires the interior and exterior line elements (1), and (2) to match smoothly at the interface. It implies that

$$e^{2\lambda_{ev}}(R_{ev}) = \left(1 - \frac{2M}{R_{ev}}\right)^{-1}, \tag{24a}$$

$$e^{2\nu_{ev}}(R_{ev}) = \left(1 - \frac{2M}{R_{ev}}\right), \tag{24b}$$

$$p_{rev}(R_{ev}) = 0. \tag{24c}$$

From the system (24), the boundary conditions become

$$(ax - 1)^4 - (ax - 1)^2 + 2aC^2(ax - 2) = 0, \tag{25a}$$

$$A^2 e^{ax} + 2ABx + B^2x^2e^{-ax} + 2aC^2x\frac{(ax - 2)}{(ax - 1)^2} - 1 = 0, \tag{25b}$$

$$\frac{\xi C^2 a^2 (a^2x^2 - 3ax + 6)^2}{(ax - 1)^6} - \Pi = 0. \tag{25c}$$

The system (25) above has six (6) unknowns; A, B, C, a, ξ, and Π in three equations. This shows that there are sufficient free parameters to satisfy the matching conditions at the boundary.

7. Physical analysis of the model

7.1. Regularity conditions

Astrophysically, valid stellar models should comply with the following conditions within the stellar interior:

(a) The energy density, radial pressure and tangential pressure should be maximum at the centre of a stellar object and monotonically decreasing towards the surface as reported in [28, 49, 61]. The radial and tangential pressures are required to have the same value at the centre of the star, that is $p_r = p_t$ when $r = 0$.

(b) The metric potentials are supposed to be positive in the interior of the stellar sphere. At the centre, it is required that $e^{2\lambda(0)} = 1$ and $e^{2\nu(0)}$ must be a positive constant [13, 16, 49].

(c) The pressure anisotropy $\triangle$ should be zero at the centre of the star as $p_r = p_t$ at this point. It can then be either increasing or decreasing function towards the surface [27, 40, 54].

7.2. Mass-radius ratio and surface redshift

The mass radius ratio for the compactness factor of the core-envelope model is defined by

$$\mu(r) = \frac{2M}{R_{ev}}. \tag{26}$$

According to Dev and Gleiser [62], and Mathias et al. [46], the compactness factor of the fluid sphere is supposed to be less than $\frac{8}{9}$, however in anisotropic spheres the compactness factor may exceed this limit. For this model, we have obtained the compactness factor equation as

$$\mu(x) = \frac{2C^2ax(ax-2)}{(ax-1)^2}. \tag{27}$$

The redshift z_s for anisotropic stellar sphere is defined to be

$$z_s(r) = \frac{1}{\sqrt{1-\mu(r)}} - 1. \tag{28}$$

The maximum redshift for anisotropic sphere needs to be ≤ 2 as stated in Mathias et al. [46], and Mafa Takisa and Maharaj [63]. For our model, the surface redshift is found to be

$$z_s = \frac{1}{\sqrt{1 - \frac{2C^2ax(ax-2)}{(ax-1)^2}}} - 1. \tag{29}$$

7.3. Zeldovich stability criteria

Zeldovich and Novikov [70] proposed stability criteria for relativistic stellar spheres as $w_r = \frac{p_r}{\rho} \leq 1$ and $w_t = \frac{p_t}{\rho} \leq 1$ to be satisfied, where w_r represents an equation of state parameter in the radial direction while w_t represents an equation of state parameter in the transverse direction. These equations are given by

$$w_{rco} = -\frac{\left(\kappa - \frac{C\gamma a\left(a^2x^2-3ax+6\right)}{(ax-1)^3}\right)(ax-1)^3}{Ca(a^2x^2-3ax+6)}, \tag{30a}$$

$$w_{tco} = \frac{(ax-1)^3}{Ca(a^2x^2-3ax+6)}\left(\frac{2Ca^2x(ax-3)}{(ax-1)^3} - \kappa + \frac{C\gamma a(a^2x^2-3ax+6)}{(ax-1)^3}\right), \tag{30b}$$

$$w_{rev} = -\frac{(ax-1)^3\left(\Pi - \frac{C^2\xi a^2\left(a^2x^2-3ax+6\right)^2}{(ax-1)^6}\right)}{Ca(a^2x^2-3ax+6)}, \tag{30c}$$

$$w_{tev} = \frac{(ax-1)^3}{Ca(a^2x^2-3ax+6)}\left(\frac{2Ca^2x(ax-3)}{(ax-1)^3} - \Pi + \frac{C^2\xi a^2(a^2x^2-3ax+6)^2}{(ax-1)^6}\right). \tag{30d}$$

7.4. Harrison–Zeldovich–Novikov stability condition

This stability condition is defined as $\frac{\partial M}{\partial \rho_0} > 0$ as stated in [13, 26, 46, 71], meaning that the stability of the star is investigated in terms of partial derivative of the mass of the relativistic stellar sphere with respect to the central energy density. The condition requires this partial derivative to be positive throughout the interior of the star. Now, using the energy density equation (18a) or (21a), at $x = 0$ we have

$$\rho_0 = -6aC, \tag{31}$$

and

$$M(\rho_0) = \frac{\rho_0^2 ax\sqrt{\frac{-6ax}{\rho_0}}(ax-2)}{36a^2(ax-1)^2}, \tag{32}$$

the function defining this condition becomes

$$\frac{\partial M}{\partial \rho_0} = \frac{ax(ax-2)}{36a^2(ax-1)^2}\left(2\rho_0\sqrt{\frac{-6ax}{\rho_0}} + \frac{3ax}{\sqrt{\frac{-6ax}{\rho_0}}}\right). \tag{33}$$

7.5. Stability via adiabatic index

The stability of the star should comply with the adiabatic index condition given by

$$\Gamma = \frac{(\rho + p_r)}{p_r}\left(\frac{p_r'}{\rho'}\right) \geq \frac{4}{3}. \tag{34}$$

The adiabatic index describes the heating behavior within relativistic stars. It provides the ratio between two specific heat capacities. For anisotropic models, it is required that

$$\Gamma \geq \Gamma_{cr} \geq \frac{4}{3}, \tag{35}$$

Bisht et al. [73], Das et al. [13], Gedela et al. [72] and Pant et al. [41], where Γ_{cr} is a critical adiabatic index given by

$$\Gamma_{cr} = \frac{4}{3} + \frac{19\mu}{21}, \tag{36}$$

where μ is a compact factor given by Eq. (27). For this model, the functions for the adiabatic indexes are found to be

$$\Gamma_{cr} = \frac{38\,C^2\,a\,x\,(ax-2)}{21\,(ax-1)^2} + \frac{4}{3}, \tag{37a}$$

$$\Gamma_{co} = -\frac{\gamma\left(\frac{Ca\left(a^2x^2-3ax+6\right)}{(ax-1)^3} - \kappa + \frac{C\gamma a\left(a^2x^2-3ax+6\right)}{(ax-1)^3}\right)}{\kappa - \frac{C\gamma a(a^2x^2-3ax+6)}{(ax-1)^3}}, \tag{37b}$$

$$\Gamma_{ev} = -\frac{2C\xi a\left(\frac{Ca\left(a^2x^2-3ax+6\right)}{(ax-1)^3} - \Pi + \frac{C^2\xi a^2\left(a^2x^2-3ax+6\right)^2}{(ax-1)^6}\right)}{(ax-1)^3} \times \frac{\left(a^4x^4 - 7a^3x^3 + 33a^2x^2 - 69ax + 90\right)}{\left(\Pi - \frac{C^2\xi a^2(a^2x^2-3ax+6)^2}{(ax-1)^6}\right)\left(a^2x^2 - 4ax + 15\right)}. \tag{37c}$$

7.6. Causality stability condition

The sound speed within relativistic stellar sphere in radial and transverse directions are defined as $v_r^2 = \frac{p_r'}{\rho'}$ and $v_t^2 = \frac{pt'}{\rho'}$. They should satisfy the conditions $0 < v_r^2 \leq 1$ and $0 < v_t^2 \leq 1$ for stable stellar objects [74, 75]. This implies that the velocity of sound should be less than that of light. The radial and transverse sound speed functions are given by

$$v_{rco}^2 = \frac{\left(\frac{3C\gamma a^2\left(a^2x^2-3ax+6\right)}{(ax-1)^4} + \frac{C\gamma a\left(-2xa^2+3a\right)}{(ax-1)^3}\right)}{\left(\frac{Ca(-2xa^2+3a)}{(ax-1)^3} + \frac{3Ca^2(a^2x^2-3ax+6)}{(ax-1)^4}\right)}, \tag{38a}$$

$$v_{rev}^2 = \frac{\frac{6C^2\xi a^3(a^2x^2-3ax+6)^2}{(ax-1)^7}}{\frac{Ca(-2xa^2+3a)}{(ax-1)^3} + \frac{3Ca^2(a^2x^2-3ax+6)}{(ax-1)^4}} + \frac{\frac{2C^2\xi a^2(-2xa^2+3a)(a^2x^2-3ax+6)}{(ax-1)^6}}{\frac{Ca(-2xa^2+3a)}{(ax-1)^3} + \frac{3Ca^2(a^2x^2-3ax+6)}{(ax-1)^4}}, \tag{38b}$$

$$v_{tco}^2 = \frac{\frac{3C\gamma a^2\left(a^2x^2-3ax+6\right)}{(ax-1)^4} - \frac{2Ca^2(ax-3)}{(ax-1)^3}}{\frac{Ca(-2xa^2+3a)}{(ax-1)^3} + \frac{3Ca^2(a^2x^2-3ax+6)}{(ax-1)^4}} + \frac{-\frac{2Ca^3x}{(ax-1)^3} + \frac{6Ca^3x(ax-3)}{(ax-1)^4} + \frac{C\gamma a\left(-2xa^2+3a\right)}{(ax-1)^3}}{\frac{Ca(-2xa^2+3a)}{(ax-1)^3} + \frac{3Ca^2(a^2x^2-3ax+6)}{(ax-1)^4}}, \tag{38c}$$

$$v_{tev}^2 = \frac{\frac{6Ca^3x(ax-3)}{(ax-1)^4} - \frac{2Ca^2(ax-3)}{(ax-1)^3}}{\frac{Ca(-2xa^2+3a)}{(ax-1)^3} + \frac{3Ca^2(a^2x^2-3ax+6)}{(ax-1)^4}} - \frac{\frac{2Ca^3x}{(ax-1)^3}}{\frac{Ca(-2xa^2+3a)}{(ax-1)^3} + \frac{3Ca^2(a^2x^2-3ax+6)}{(ax-1)^4}} + \frac{\frac{6C^2\Pi a^3\left(a^2x^2-3ax+6\right)^2}{(ax-1)^7}}{\frac{Ca(-2xa^2+3a)}{(ax-1)^3} + \frac{3Ca^2(a^2x^2-3ax+6)}{(ax-1)^4}} + \frac{\frac{2C^2\Pi a^2\left(-2xa^2+3a\right)\left(a^2x^2-3ax+6\right)}{(ax-1)^6}}{\frac{Ca(-2xa^2+3a)}{(ax-1)^3} + \frac{3Ca^2(a^2x^2-3ax+6)}{(ax-1)^4}}. \tag{38d}$$

7.7. Herrera cracking stability condition

For the interior region of an anisotropic sphere to be stable, it must satisfy the following condition given in Herrera [76]

$$|v_t^2 - v_r^2| < 1. \tag{39}$$

For this case the equations of this condition are defined as

$$v_{tco}^2 - v_{rco}^2 = \frac{\frac{3C\gamma a^2(a^2x^2-3ax+6)}{(ax-1)^4} - \frac{2Ca^2(ax-3)}{(ax-1)^3}}{\frac{Ca(-2xa^2+3a)}{(ax-1)^3} + \frac{3Ca^2(a^2x^2-3ax+6)}{(ax-1)^4}} + \frac{-\frac{2Ca^3x}{(ax-1)^3} + \frac{6Ca^3x(ax-3)}{(ax-1)^4} + \frac{C\gamma a(-2xa^2+3a)}{(ax-1)^3}}{\frac{Ca(-2xa^2+3a)}{(ax-1)^3} + \frac{3Ca^2(a^2x^2-3ax+6)}{(ax-1)^4}} - \frac{\frac{3C\gamma a^2(a^2x^2-3ax+6)}{(ax-1)^4} + \frac{C\gamma a(-2xa^2+3a)}{(ax-1)^3}}{\frac{Ca(-2xa^2+3a)}{(ax-1)^3} + \frac{3Ca^2(a^2x^2-3ax+6)}{(ax-1)^4}}, \tag{40a}$$

$$v_{rco}^2 - v_{tco}^2 = \frac{\frac{3C\gamma a^2(a^2x^2-3ax+6)}{(ax-1)^4} + \frac{C\gamma a(-2xa^2+3a)}{(ax-1)^3}}{\frac{Ca(-2xa^2+3a)}{(ax-1)^3} + \frac{3Ca^2(a^2x^2-3ax+6)}{(ax-1)^4}} - \frac{\frac{3C\gamma a^2(a^2x^2-3ax+6)}{(ax-1)^4} - \frac{2Ca^2(ax-3)}{(ax-1)^3}}{\frac{Ca(-2xa^2+3a)}{(ax-1)^3} + \frac{3Ca^2(a^2x^2-3ax+6)}{(ax-1)^4}} + \frac{-\frac{2Ca^3x}{(ax-1)^3} + \frac{6Ca^3x(ax-3)}{(ax-1)^4} + \frac{C\gamma a(-2xa^2+3a)}{(ax-1)^3}}{\frac{Ca(-2xa^2+3a)}{(ax-1)^3} + \frac{3Ca^2(a^2x^2-3ax+6)}{(ax-1)^4}}, \tag{40b}$$

$$v_{tev}^2 - v_{rev}^2 = \frac{\frac{6Ca^3x(ax-3)}{(ax-1)^4} - \frac{2Ca^2(ax-3)}{(ax-1)^3}}{\frac{Ca(-2xa^2+3a)}{(ax-1)^3} + \frac{3Ca^2(a^2x^2-3ax+6)}{(ax-1)^4}} + \frac{-\frac{2Ca^3x}{(ax-1)^3} + \frac{6C^2\xi a^3(a^2x^2-3ax+6)^2}{(ax-1)^7}}{\frac{Ca(-2xa^2+3a)}{(ax-1)^3} + \frac{3Ca^2(a^2x^2-3ax+6)}{(ax-1)^4}} + \frac{\frac{2C^2\xi a^2(-2xa^2+3a)(a^2x^2-3ax+6)}{(ax-1)^6}}{\frac{Ca(-2xa^2+3a)}{(ax-1)^3} + \frac{3Ca^2(a^2x^2-3ax+6)}{(ax-1)^4}}, \tag{40c}$$

$$v_{rev}^2 - v_{tev}^2 = \frac{\frac{6C^2\xi a^3(a^2x^2-3ax+6)^2}{(ax-1)^7}}{\frac{Ca(-2xa^2+3a)}{(ax-1)^3} + \frac{3Ca^2(a^2x^2-3ax+6)}{(ax-1)^4}} + \frac{\frac{2C^2\xi a^2(-2xa^2+3a)(a^2x^2-3ax+6)}{(ax-1)^6}}{\frac{Ca(-2xa^2+3a)}{(ax-1)^3} + \frac{3Ca^2(a^2x^2-3ax+6)}{(ax-1)^4}} - \frac{\frac{6Ca^3x(ax-3)}{(ax-1)^4} - \frac{2Ca^2(ax-3)}{(ax-1)^3} - \frac{2Ca^3x}{(ax-1)^3}}{\frac{Ca(-2xa^2+3a)}{(ax-1)^3} + \frac{3Ca^2(a^2x^2-3ax+6)}{(ax-1)^4}}. \tag{40d}$$

7.8. Energy conditions

Energy conditions must be met by relativistic stellar objects for stability. Different researchers such as Gedela et al. [72], Sunzu and Mathias [77], and Maurya et al. [78] discussed different conditions including weak energy condition (WEC), null energy condition (NEC), strong energy condition (SEC), and dominant energy condition (DEC) defined as

$$WEC: \rho \geq 0,\ \ \rho + p_r \geq 0,\ \ \rho + p_t \geq 0, \tag{41a}$$

$$NEC: \rho + p_t \geq 0,\ \ \rho + p_r \geq 0, \tag{41b}$$

$$SEC: \rho + p_t \geq 0,\ \ \rho + p_r \geq 0,\ \ \rho + 2p_t + p_r \geq 0, \tag{41c}$$

$$DEC: \rho \geq 0,\ \ \rho - p_t \geq 0,\ \ \rho - p_r \geq 0. \tag{41d}$$

These conditions imply that the energy behavior within the stellar interior is positive throughout.

Table 1 Stellar masses and radii for known stars

a	C	R	$\frac{M}{M_\odot}$	Star	References
−0.022	0.450	9.13	1.29	SMCX-1	[64]
−0.021	0.5170	6.70	0.98	HerX-1	[65]
−0.021	0.5145	7.80	1.31	EXO1745-248	[66]
−0.021	0.4940	9.70	1.76	VelaX-1	[64]
−0.021	0.5460	8.20	1.85	4U1608-52	[67]
−0.021	0.4838	6.20	0.7	SAXJ1808.4-3658	[68]
−0.01365	0.5400	9.10	1.63	PSRJ1903+0327	[69]

Table 2 Central density, pressures, adiabatic indexes, and maximum compactness factor, and surface redshift

$\rho(r=0)$	$p_r\&p_t(r=0)$	$\Gamma_{cr}(r=0)$	$\Gamma(r=0)$	$\mu_{\max}$	$z_{s\max}$
0.0684	0.0201	1.3333	1.7763	0.2256	0.1364

7.9. Equilibrium of the natural forces

The condition of equilibrium describes the behavior of the natural physical forces within the star. These forces are gravitational force (F_g), hydrostatic force (F_h), and anisotropic force (F_a). For a relativistic stellar object to be stable, these forces should balance. To investigate the state of forces equilibrium, we use the Tolman–Oppenheimer–Volkoff (TOV) equation initiated by Tolman [79] and Oppenheimer and Volkoff [80], which is given by

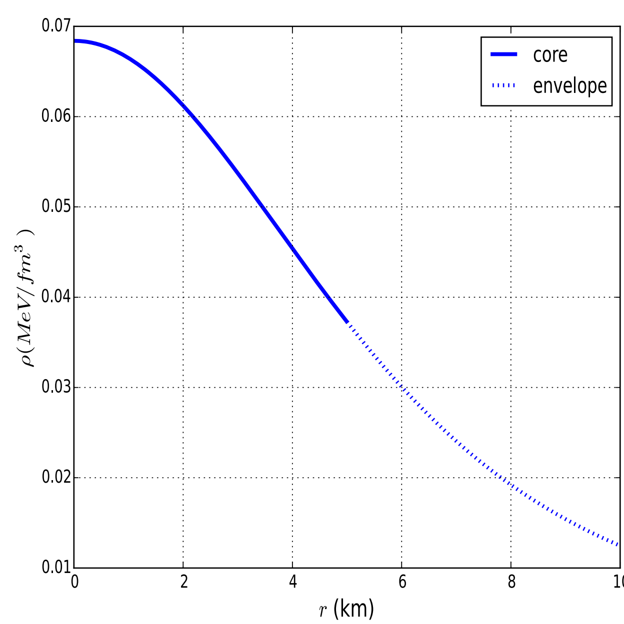

Fig. 1 Plot of energy density against radial coordinate. Constant values used are: $a = -0.03, C = 0.38$

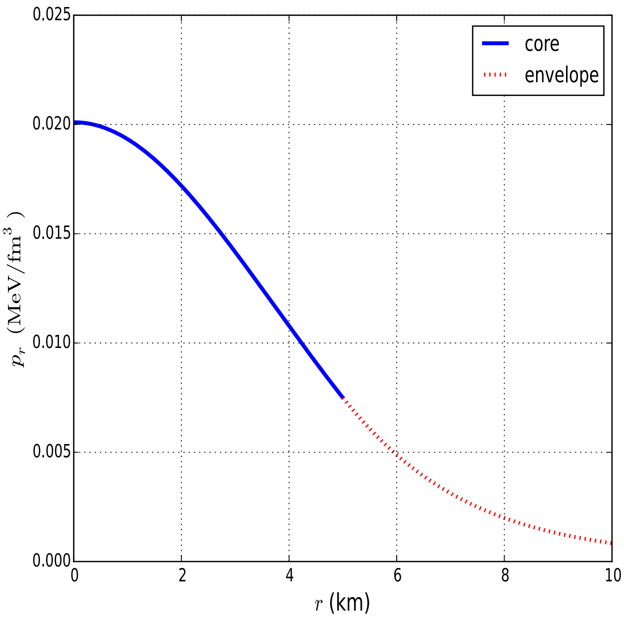

Fig. 2 Plot of radial pressure against radial coordinate. Constant values used are: $a = -0.03, C = 0.38, \gamma = 0.405, \kappa = 0.0076, \xi = 5.4, \Pi = 1 \times 10^{-15}$

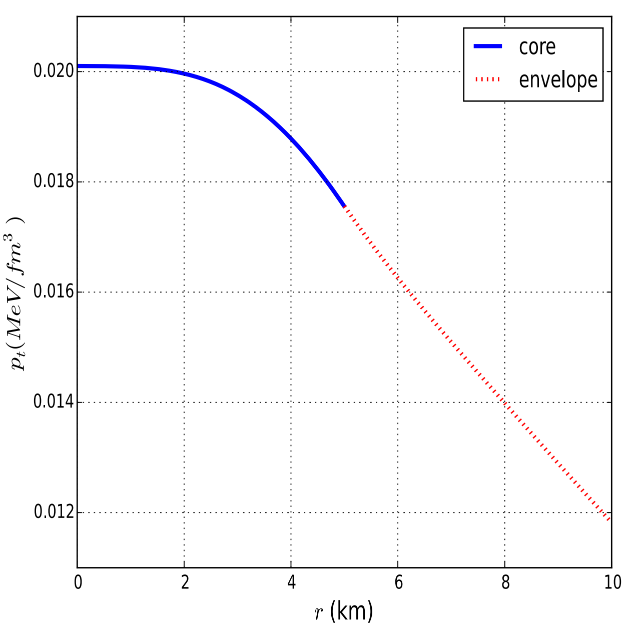

Fig. 3 Plot of tangential pressure against radial coordinate. Constant values used are: $a = -0.03, C = 0.38, \gamma = 0.405, \kappa = 0.0076, \xi = 5.4, \Pi = 1 \times 10^{-15}$

$$\frac{-M_g(\rho + p_r)}{r^2} e^{\lambda - \nu} - \frac{dp_r}{dr} + \frac{2\Delta}{r} = 0, \tag{42}$$

where $M_g = \frac{r^2 \nu' e^{\nu - \lambda}}{2}$ defines the effective gravitational mass. Then, Eq. (42) modifies to

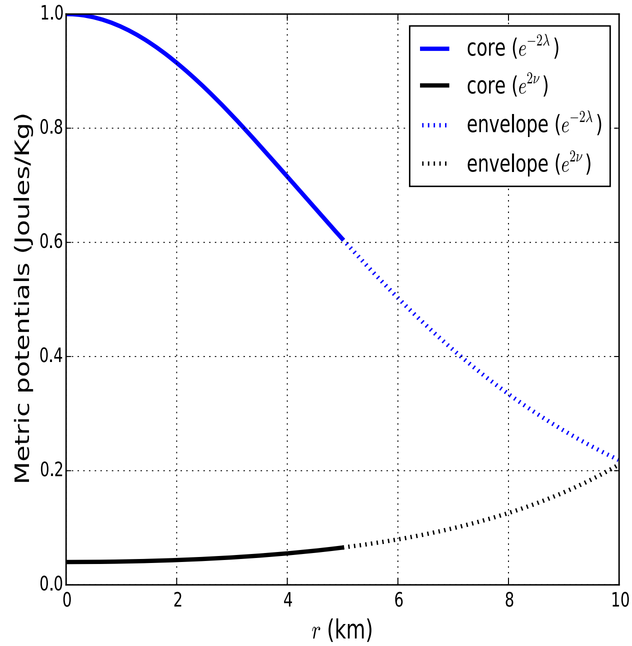

Fig. 4 Plot of metric potentials against radial coordinate. Constant values used are: $a = -0.03, C = 0.38, A = 0.04, B = 0.0028$

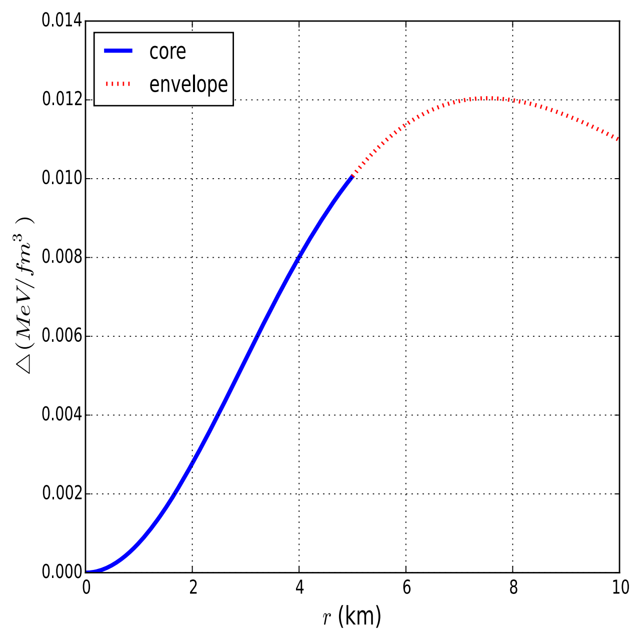

Fig. 5 Plot of measure of anisotropy against radial coordinate. Constant values used are: $a = -0.03, C = 0.38, \gamma = 0.405, \kappa = 0.0076, \xi = 5.4, \Pi = 1 \times 10^{-15}$

$$\frac{-\nu'}{2}(\rho + p_r) - \frac{dp_r}{dr} + \frac{2}{r}\Delta = 0, \tag{43}$$

where

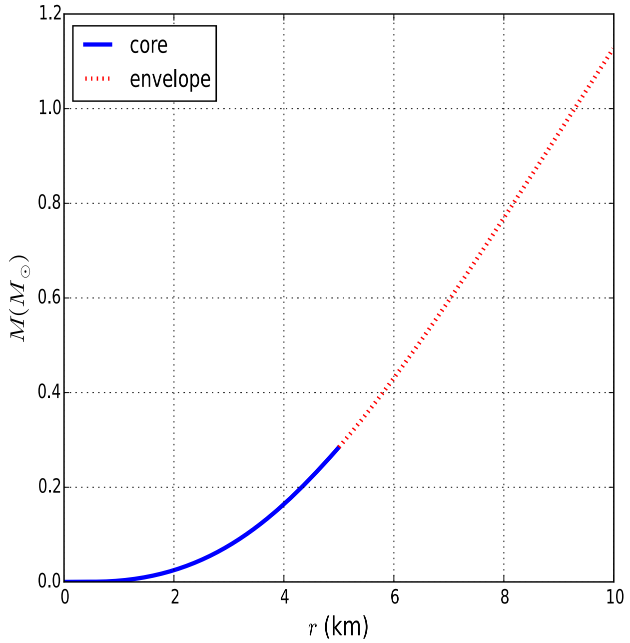

Fig. 6 Plot of mass against radial coordinate. Constant values used are: $a = -0.03, C = 0.38$

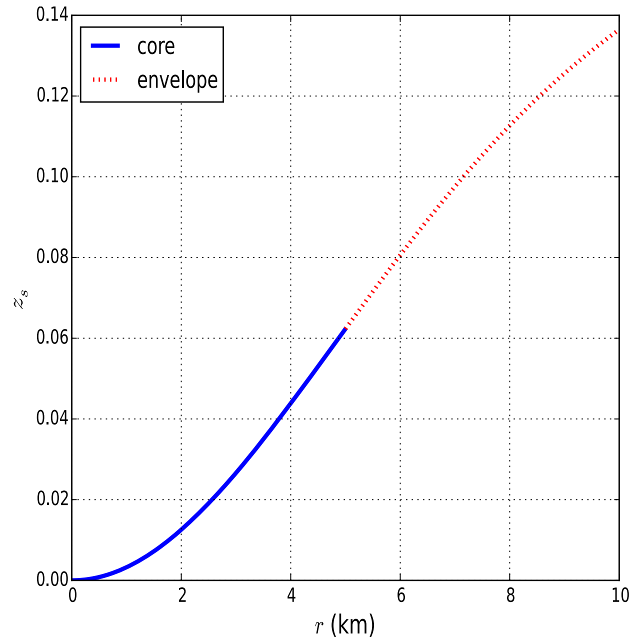

Fig. 8 Surface redshift against radial coordinate. Constant values used are: $a = -0.03, C = 0.38$

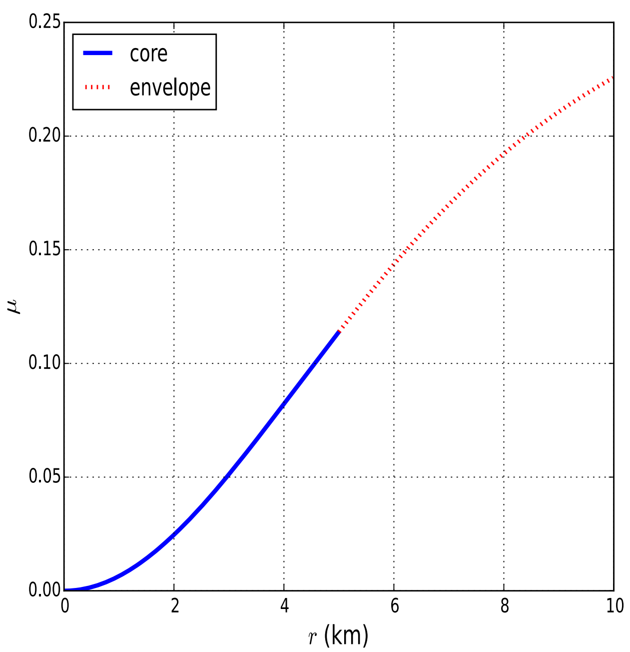

Fig. 7 Plot of mass to radius ratio against radial coordinate. Constant values used are: $a = -0.03, C = 0.38$

$$F_g = \frac{-\nu'}{2}(\rho + p_r), \tag{44a}$$

$$F_h = -\frac{dp_r}{dr}, \tag{44b}$$

$$F_a = \frac{2}{r}\Delta. \tag{44c}$$

In our model, the functions for the natural forces are given by

$$F_{gco} = -\frac{C\left(\frac{x}{C}\right)^{1/2}(2B - Bax + Aae^{ax})}{2(Bx + Ae^{ax})} \times \left(\frac{Ca(a^2x^2 - 3ax + 6)}{(ax-1)^3} - \kappa + \frac{C\gamma a(a^2x^2 - 3ax + 6)}{(ax-1)^3}\right), \tag{45a}$$

$$F_{hco} = 2C\sqrt{\frac{x}{C}}\left(\frac{3C\gamma a^2(a^2x^2 - 3ax + 6)}{(ax-1)^4} + \frac{C\gamma a(3a - 2a^2x)}{(ax-1)^3}\right), \tag{45b}$$

$$F_{aco} = \frac{4Ca^2x(ax-3)}{\sqrt{\frac{x}{C}}(ax-1)^3}, \tag{45c}$$

$$F_{gev} = \frac{C\left(\frac{x}{C}\right)^{1/2}(2B - Bax + Aae^{ax})}{2(Bx + Ae^{ax})} \times \left(\frac{Ca(a^2x^2 - 3ax + 6)}{(ax-1)^3} - \Pi + \frac{C^2\xi a^2(a^2x^2 - 3ax + 6)^2}{(ax-1)^6}\right), \tag{45d}$$

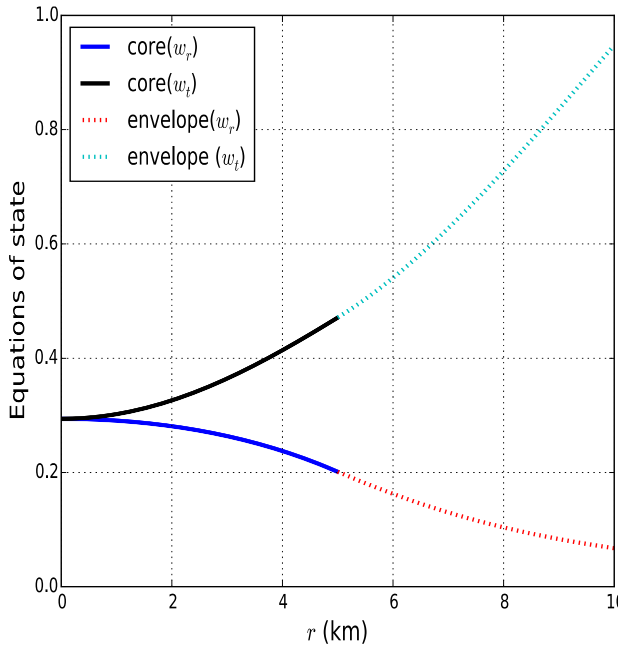

Fig. 9 Plot of equations of state parameters against radial coordinate. Constant values used are: $a = -0.03, C = 0.38, \gamma = 0.405, \kappa = 0.0076, \xi = 5.4, \Pi = 1 \times 10^{-15}$

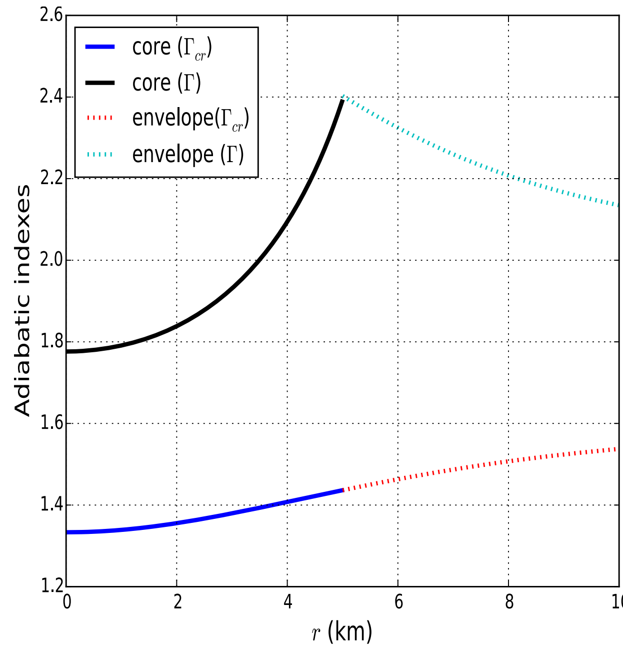

Fig. 11 Plot of adiabatic indexes against radial coordinate. Constant values used are: $a = -0.03, C = 0.38, \gamma = 0.405, \kappa = 0.0076, \xi = 5.4, \Pi = 1 \times 10^{-15}$

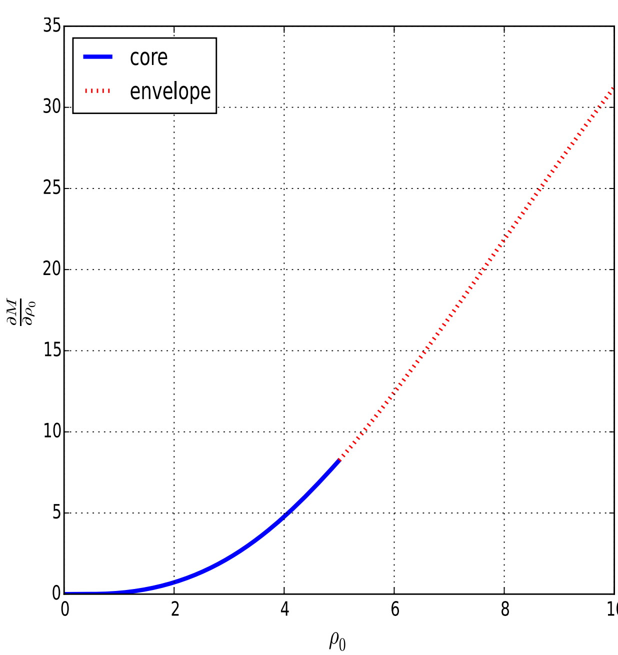

Fig. 10 Plot of partial derivative of mass with respect to central energy density against radial coordinate. Constant values used are: $a = -0.03, C = 0.38$

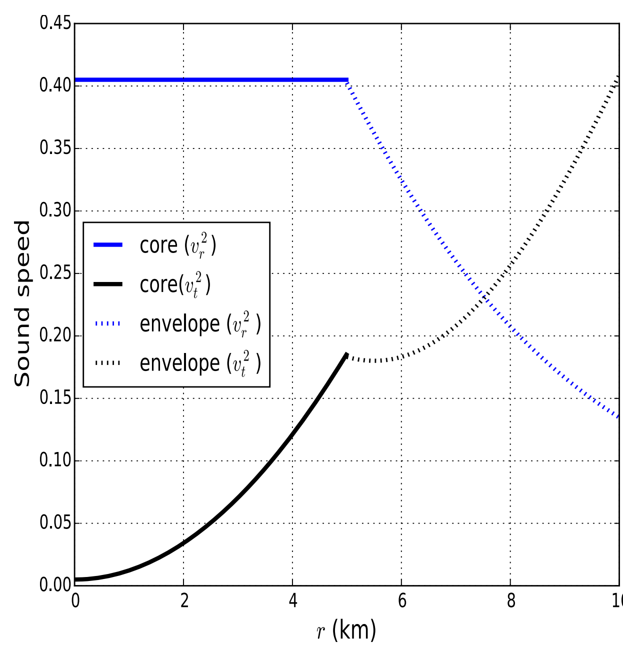

Fig. 12 Plot of square of radial and tangential speed of sound against radial coordinate. Constant values used are: $a = -0.03, C = 0.38, \gamma = 0.405, \kappa = 0.0076, \xi = 5.4, \Pi = 1 \times 10^{-15}$

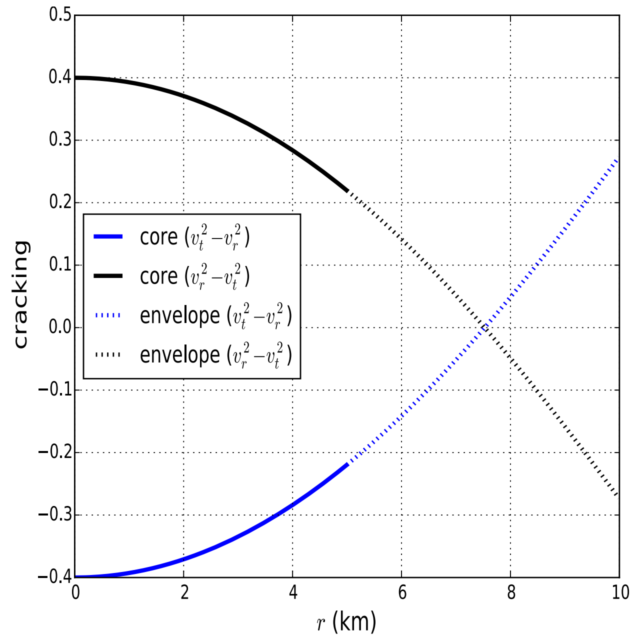

Fig. 13 Plot of square differences of radial and tangential speed of sound against radial coordinate. Constant values used are: $a = -0.03, C = 0.38, \gamma = 0.405, \kappa = 0.0076, \xi = 5.4, \Pi = 1 \times 10^{-15}$

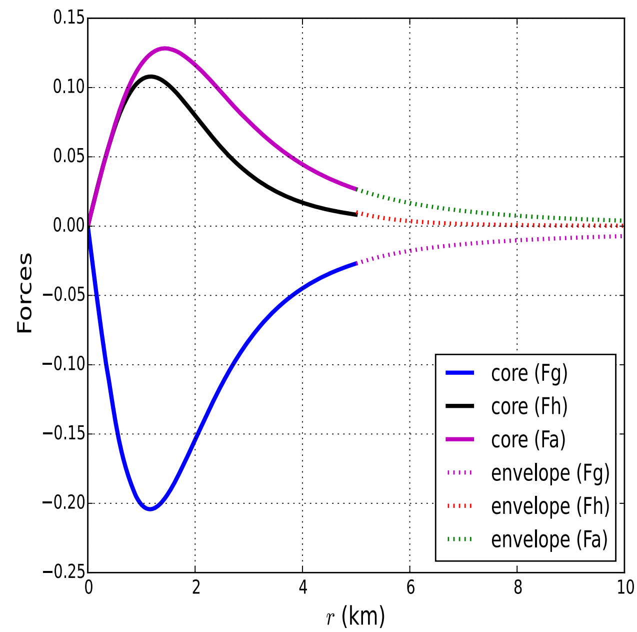

Fig. 15 Plot of natural forces against radial coordinate. Constant values used are: $a = -0.03, C = 0.38, \gamma = 0.405, \kappa = 0.0076, \xi = 5.4, \Pi = 1 \times 10^{-15}, A = 0.04, B = 0.0028$

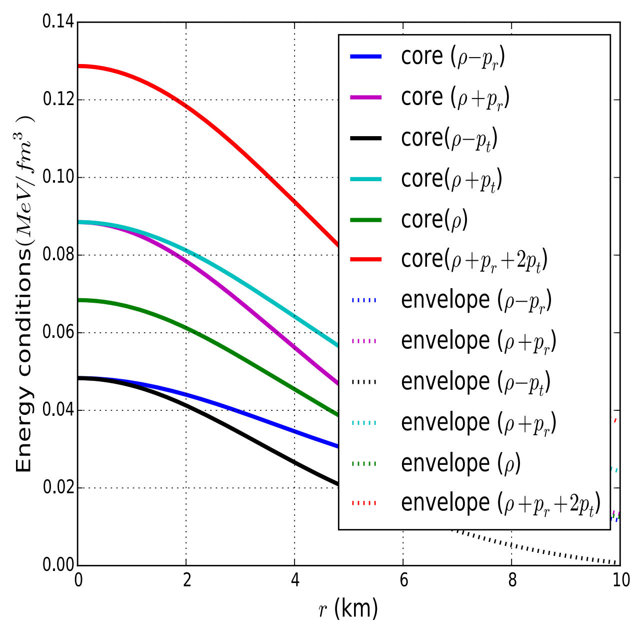

Fig. 14 Plot of energy conditions against radial coordinate. Constant values used are: $a = -0.03, C = 0.38, \gamma = 0.405, \kappa = 0.0076, \xi = 5.4, \Pi = 1 \times 10^{-15}$

$$F_{hev} = 2C\sqrt{\frac{x}{C}}\left(\frac{6C^2\xi a^3(a^2x^2 - 3ax + 6)^2}{(ax-1)^7} + \frac{2C^2\xi a^2(3a - 2a^2x)}{(ax-1)^6}(a^2x^2 - 3ax + 6)\right), \tag{45e}$$

$$F_{aev} = \frac{4Ca^2x(ax-3)}{\sqrt{\frac{x}{C}}(ax-1)^3}. \tag{45f}$$

The stellar sphere is said to be in state of equilibrium when

$$F_h + F_g + F_a = 0. \tag{46}$$

8. Discussion

We have developed a core-envelope stellar model admitting conformal symmetry via equations of state. The core is described by a linear equation of state having a radius assumed to range from 0 to 5 km while the envelope obeys a quadratic equation of state with radius from 5 to 10 km. MATLAB software has been used for mathematical computations while Python was employed in graphical plotting. We have specified a number of parameter values as indicated in each figure on physical grounds so that a well behaved model is generated. In our specification, $\Pi = 1 \times 10^{-15}$ which is very small due to the fact that the pressure should vanish at the surface. A greater value of Π can prevent this condition from being met. Also, in the absence of matter ($\rho = 0$) in Eq. (20), the pressure should also be zero. A greater value of Π would imply a non-zero pressure in vacuum, which is nonphysical. This also resulted in obtaining masses and radii consistent with different observed stars such as PSRJ1903+0327, SAXJ1808.4-3658, 4U1608-52, VelaX-1, HerX-1, SMCX-1, and EXO1785-248 as indicated in Table 1. We have also analyzed several physical requirements for relativistic compact star models. The regularity condition is satisfied, the mass-radius ratio and surface redshift are found to be within the range of observed stars as indicated in Table 2. We further checked for stability of our stellar model via Zeldovich criterion, Harrison-Zeldovich-Novikov condition, adiabatic index, causality, cracking, energy conditions, and equilibrium of forces. The results are graphically presented in different figures and found to be physically valid and comply to astrophysical needs.

It is indicated in Figs. 1, 2 and 3 that the energy density, radial pressure and tangential pressure are continuous functions with maximum values at the centre while monotonically decreasing towards the surface. Similar profiles have been found by [25, 61, 81]. Figure 4 indicates that the metric functions are continuous and positive about the interior of the core-envelope star with $e^{-2\lambda} = 1$ and $e^{2\nu} = 0.04$ at the centre. These behaviors are necessary for relativistic core-envelope models with physical significance. Figure 5 describes the behavior of the anisototropic pressure as a continuous increasing function from the centre to the surface with zero value at the centre as the radial and tangential pressures are equal at this point. These profiles are similar to those generated in Mafa Takisa et al. [42], and Christopher et al. [54].

The mass of the core-envelope star is positive, continuous and it is increasing function against the radial distance as demonstrated in Fig. 6. The mass-radius ratio (compactness factor) behavior is indicated in Fig. 7. It is a continuous increasing function as radius increases, such that $\mu_{max} = 0.2256 < \frac{8}{9}$ as required. The surface redshift z_s in Fig. 8 satisfies the condition $z_s \leq 2$ with maximum value of 0.1364 as given in Table 2. Similar features are found in [13, 26, 82].

Figure 9 shows that the equation of state parameters in radial and tangential directions are such that $w_r < 1$ and $w_t < 1$, respectively as required. Figure 10 shows that the Harrison–Zeldovich–Novikov stability condition is well satisfied as $\frac{\partial M}{\partial \rho_0} > 0$. Figure 11 shows that the adiabatic indexes are such that $\Gamma \geq \Gamma_{cr} \geq \frac{4}{3}$ as needed with the central minimum values be, $\Gamma(r = 0) = 1.7763 \geq \Gamma_{cr} = 1.3333$ as shown in Table 2. Figure 12 indicates that the speed of sound is positive and less than the speed of light. These profiles are also found in models generated by Sagar et al. [74], Lighuda et al. [83], Olengeile et al. [84], and Upreti et al. [85]. Figure 13 elaborate the cracking condition, which is well behaved as required.

Figure 14 shows that the energy conditions are all positive about the interior of the core-envelope star as required. Figure 15 details the balance of the equilibrium of natural forces within a relativistic stellar object. These behaviors are similar to those observed by Mathias et al. [25, 46]. It is clear that the satisfaction of all these relativistic conditions indicates that our generated class of solution for the core-envelope compact star model is astrophysically significance.

Acknowledgements We acknowledge The University of Dodoma-Tanzania for providing conducive and supportive environment to conduct research. YKK thanks the employer and sponsor, Mbeya University of Science and Technology (MUST)-Tanzania for financial support.

References

[1] G G L Nashed and S Capozziello *Eur. Phys. J. C* **81** 481 (2021). https://doi.org/10.1140/epjc/s10052-021-09273-8

[2] K Pant and P Fuloria, New Astron. **84** (2021). https://doi.org/10.1016/j.newast.2020.101509

[3] E J A Curi, L B Castro, C V Flores and C H Lenzi *Eur. Phys. J. C* **82** 527 (2022). https://doi.org/10.1140/epjc/s10052-022-10498-4

[4] S Das, R Sharma, K Chakraborty and L Baskey *Gen Relativ. Gravit.* **52** 101 (2020). https://doi.org/10.1007/s10714-020-02753-4

[5] P Mafa Takisa, S D Maharaj and L L Leeuw, Eur. Phys. J. C **79** 8 (2019). https://doi.org/10.1140/epjc/s10052-018-6519-0

[6] I Noureen, S A Mardan, M Azam, W Shahzad and S Khalid *Eur. Phys. J. C* **79** 302 (2019). https://doi.org/10.1140/epjc/s10052-019-6806-4

[7] R Patel, B S Ratanpal and D M Pandya *Astrophys. Space Sci.* **368** 58 (2023). https://doi.org/10.1007/s10509-023-04213-2

[8] N Sarkar, K N Singh, S Sarkar and F Rahaman *Eur. Phys. J. C* **79** 516 (2019). https://doi.org/10.1140/epjc/s10052-019-7035-6

[9] L Suleiman, M Fortin, J L Zdunik and C Providencia *Phys. Rev. C* **106** 035805 (2022). https://doi.org/10.1103/PhysRevC.106.035805

[10] A K Prasad, J Kumar and A Sarkar *Gen. Relativ. Gravit.* **53** 108 (2021). https://doi.org/10.1007/s10714-021-02883-3

[11] S K Maurya and F Tello-Ortiz *Eur. Phys. J. C* **79** 33 (2019). https://doi.org/10.1140/epjc/s10052-019-6575-0

[12] D Kileba Matondo and S D Maharaj, Entropy **23** 1406 (2021). https://doi.org/10.3390/e23111406

[13] S Das, K N Singh, L Baskey, F Rahaman and A K Aria *Gen. Relativ. Gravit.* **53** 25 (2021). https://doi.org/10.1007/s10714-021-02792-5

[14] V V Usov *Phys. Rev. D* **70** 067301 (2004). https://doi.org/10.1103/PhysRevD.70.067301

[15] F Weber *Pulsars as Astrophysical Laboratories for Nuclear and Particle Physics* (Routledge) (2017) https://doi.org/10.1201/9780203741719
[16] A T Abdalla, J M Sunzu and J M Mkenyeleye *Pramana* **95** 86 (2021). https://doi.org/10.1007/s12043-021-02096-y
[17] J M Sunzu and M Thomas *Pramana* **91** 75 (2018). https://doi.org/10.1007/s12043-018-1650-x
[18] F Weber, Prog. Part. Nucl. Phys. **54** (2005). https://doi.org/10.1016/j.ppnp.2004.07.001
[19] L Herrera and W Barreto *Phys. Rev. D* **88** 084022 (2013). https://doi.org/10.1103/PhysRevD.88.084022
[20] M Malaver and M Esculpi arXiv:2310.01730 [gr-qc] (2023)
[21] M Malaver and R Iyer arXiv:2310.00859 [gr-qc] (2023)
[22] M Malaver and R Iyer, Univ. J. Phys. Res. **2** (2023). https://doi.org/10.31586/ujpr.2023.748
[23] M Malaver and R Iyer arXiv:2303.12161 [gr-qc] (2023)
[24] M Malaver and R Iyer arXiv:2204.13108 [gr-qc] (2022)
[25] A V Mathias, J M Mkenyeleye and J M Sunzu *New Astron.* **110** 102216 (2024). https://doi.org/10.1016/j.newast.2024.102216
[26] S K Maurya, S D Maharaj, J Kumar and A K Prasad *Gen. Relativ. Gravit.* **51** 86 (2019). https://doi.org/10.1007/s10714-019-2570-x
[27] R Sharma, A Ghosh, S Bhattacharya and S Das *Eur. Phys. J. C* **81** 527 (2021). https://doi.org/10.1140/epjc/s10052-021-09310-6
[28] J W Jape, S D Maharaj, J M Sunzu, and J M Mkenyeleye, Indian J. Phys. **97** (2023). https://doi.org/10.1007/s12648-022-02521-x
[29] R N Nasheeha, S Thirukkanesh, and F C Ragel, Indian J. Phys. **98** (2024). https://doi.org/10.1007/s12648-023-02857-y
[30] S Thirukkanesh and S D Maharaj *Class. Quantum Grav.* **25** 235001 (2008). https://doi.org/10.1088/0264-9381/25/23/235001
[31] E Babichev, V Dokuchaev and Y Eroshenko *Class. Quantum Grav.* **22** 143 (2004). https://doi.org/10.1088/0264-9381/22/1/010
[32] P Bhar, M Govender and R Sharma *Pramana* **90** 5 (2018). https://doi.org/10.1007/s12043-017-1500-2
[33] J Estevez-Delgado, N E R Maya, J M Pena, A Cleary-Balderas and J M Paulin-Fuentes *Mod. Phys. Lett. A* **36** 2150153 (2021). https://doi.org/10.1142/S0217732321501534
[34] S Thirukkanesh and F C Ragel, Pramana **83**, (2014). https://doi.org/10.1007/s12043-014-0766-x
[35] M Malaver, Am. J. Astron. Astrophys. **1** (2013). https://doi.org/10.11648/j.ajaa.20130104.11
[36] M Malaver World Appl. Program. **3** (2013)
[37] M Malaver and H D Kasmaei ,Int. J. Astrophys. Space Sci. **7** (2019). https://doi.org/10.11648/j.ijass.20190705.11
[38] J M Sunzu and A V Mathias, Indian J. Phys. **97** (2022). https://doi.org/10.1007/s12648-022-02455-4
[39] J M Sunzu and A S Lighuda *New Astron.* **100** 101977 (2023). https://doi.org/10.1016/j.newast.2022.101977
[40] S A Mardan, I Noureen and A Khalid *Eur. Phys. J. C* **81** 912 (2021). https://doi.org/10.1140/epjc/s10052-021-09710-8
[41] R P Pant, S Gedela, R K Bisht and N Pant *Eur. Phys. J. C* **79** 602 (2019). https://doi.org/10.1140/epjc/s10052-019-7098-4
[42] P Mafa Takisa, S D Maharaj, and C Mulangu, Pramana **92** 40 (2019). https://doi.org/10.1007/s12043-018-1695-x
[43] M K Jasim, S K Maurya, A Errehymy, A K Jassim, K S Nisar and A Abdel-Aty *Chin. Phys. C* **48** 075108 (2024). https://doi.org/10.1088/1674-1137/ad3e67
[44] S K Maurya and R Nag *Eur. Phys. J. C* **82** 48 (2022). https://doi.org/10.1140/epjc/s10052-021-09972-2
[45] S. K. Maurya, K. Newton Singh, A. Errehymy, and M. Daoud ,Eur. Phys. J. Plus **135** 824 (2020). https://doi.org/10.1140/epjp/s13360-020-00832-8
[46] A V Mathias, J M Sunzu and J M Mkenyeleye *New Astron.* **106** 102115 (2024). https://doi.org/10.1016/j.newast.2023.102115
[47] A Ditta, X Tiecheng, S K Maurya, G Mustafa, A Mahmood and S Ray *Nucl. Phys. B* **1007** 116689 (2024). https://doi.org/10.1016/j.nuclphysb.2024.116689
[48] K N Singh, S K Maurya, S Gedela and R K Bisht ,J. High Energy Astrophys. **42** (2024). https://doi.org/10.1016/j.jheap.2024.04.008
[49] S K Maurya, S D Maharaj and D Deb *Eur. Phys. J. C* **79** 170 (2019). https://doi.org/10.1140/epjc/s10052-019-6677-8
[50] J W Jape, S D Maharaj, J M Sunzu and J M Mkenyeleye *Eur. Phys. J. C* **81** 1057 (2021). https://doi.org/10.1140/epjc/s10052-021-09856-5
[51] A M Manjonjo, S D Maharaj and S Moopanar *Eur. Phys. J. Plus* **132** 62 (2017). https://doi.org/10.1140/epjp/i2017-11309-0
[52] A M Manjonjo, S D Maharaj and S Moopanar *J. Phys. Commun.* **3** 025003 (2019). https://doi.org/10.1088/2399-6528/aaf3cb
[53] J W Jape, J M Sunzu, S D Maharaj, and J M Mkenyeleye, Indian J. Phys. **97** (2023). https://doi.org/10.1007/s12648-022-02468-z
[54] J Christopher, J W Jape and J M Sunzu *Int. J. Mod. Phys. D* **33** 2450022 (2024). https://doi.org/10.1142/S0218271824500226
[55] S D Maharaj, R Maartens and M S Maharaj ,Int. J. Theor. Phys. **34** (1995). https://doi.org/10.1007/BF00673843
[56] L Herrera, A D Prisco, J Ospino, and E Fuenmayor ,J. Math. Phys. **42** (2001). https://doi.org/10.1063/1.1364503
[57] M C Durgapal and R Bannerji *Phys. Rev. D* **27** 328 (1983). https://doi.org/10.1103/PhysRevD.27.328
[58] S K Maurya Ksh N Singh, S V Lohakare and B Mishra, *Fortschr. Phys.* **70** 2200061 (2022). https://doi.org/10.1002/prop.202200061
[59] S K Maurya Ksh N Singh, M Govender and S Hansraj *Astrophys. J.* **925** 208 (2022). https://doi.org/10.3847/1538-4357/ac4255
[60] S K Maurya and G Mustafa M Govender and Ksh N Singh *J. Cosmol. Astropart. Phys.* **2022** 003 (2022). https://doi.org/10.1088/1475-7516/2022/10/003
[61] S Thirukkanesh, R Sharma and S Das *Eur. Phys. J. Plus* **135** 629 (2020). https://doi.org/10.1140/epjp/s13360-020-00653-9
[62] K Dev and M Gleiser ,Gen. Relativ. Gravit. **34** (2002). https://doi.org/10.1023/A:1020707906543
[63] P Mafa Takisa and S D Maharaj ,Astrophys. Space Sci. **361** 262 (2016). https://doi.org/10.1007/s10509-016-2840-y
[64] M L Rawls, J A Orosz, J E McClintock, M A Torres, C D Bailyn and M M Buxton *Astrophys. J.* **730** 25 (2011). https://doi.org/10.1088/0004-637X/730/1/25
[65] X-D Li, Z-G Dai and Z-R Wang *Astron. Astrophys.* **303** L1 (1995).
[66] F Ozel, T Guver and D Psaltis *Astrophys. J.* **693** 1775 (2009). https://doi.org/10.1088/0004-637X/693/2/1775
[67] T Güver Fözel, A Cabrera-Lavers, and P Wroblewski *Astrophys. J.* **712** 964 (2010). https://doi.org/10.1088/0004-637X/712/2/964
[68] P Elebert, M T Reynolds, P J Callanan, D J Hurley, G Ramsay, F Lewis, D Russell, B Nord, S Kane, D DePoy et al. ,Mon. Not. R. Astron. Soc. **395** (2009). https://doi.org/10.1111/j.1365-2966.2009.14562.x
[69] P C C Freire, C G Bassa, N Wex, I H Stairs, D J Champion, S M Ransom, P Lazarus, V M Kaspi, J W T Hessels, M Kramer et al., Mon. Not. R. Astron. Soc. **412** (2011). https://doi.org/10.1111/j.1365-2966.2010.18109.x
[70] Y B Zeldovich and I D Novikov ,Relativistic Astrophysics. Vol. 1: Stars and Relativity (Chicago: University of Chicago Press) (1971)
[71] B K Harrison, K S Thorne, M Wakano, and J A Wheeler, Gravitation Theory and Gravitational Collapse (1965)
[72] S Gedela, N Pant, J Upreti and R P Pant *Eur. Phys. J. C* **79** 566 (2019). https://doi.org/10.1140/epjc/s10052-019-7074-z

[73] R K Bisht, S Gedela, N Pant and N Tewari *Res. Astron. Astrophys.* **21** 162 (2021). https://doi.org/10.1088/1674-4527/21/7/162
[74] K G Sagar, N Pant and B Pandey *Phys. Dark Univ.* **35** 101125 (2022). https://doi.org/10.1016/j.dark.2022.101125
[75] A Banerjee, S Banerjee, S Hansraj and A Övgün *Eur. Phys. J. Plus* **132** 130 (2017). https://doi.org/10.1140/epjp/i2017-11413-1
[76] L Herrera ,Phys. Lett. A **165** (1992). https://doi.org/10.1016/0375-9601(92)90036-L
[77] J M Sunzu and A V Mathias ,Indian J. Phys. **97** (2022). https://doi.org/10.1007/s12648-022-02455-4
[78] S K Maurya, A Errehymy, B Dayanandan, S Ray, N Al-Harbi and A-H Abdel-Aty *Eur. Phys. J. C* **83** 532 (2023). https://doi.org/10.1140/epjc/s10052-023-11695-5
[79] R C Tolman *Phys. Rev.* **55** 364 (1939). https://doi.org/10.1103/PhysRev.55.364
[80] J R Oppenheimer and G M Volkoff *Phys. Rev.* **55** 374 (1939). https://doi.org/10.1103/PhysRev.55.374
[81] D Bhattacharjee and P K Chattopadhyay *Eur. Phys. J. C* **84** 77 (2024). https://doi.org/10.1140/epjc/s10052-024-12449-7
[82] S K Maurya, A Banerjee, M K Jasim, J Kumar, A K Prasad and A Pradhan *Phys. Rev. D* **99** 044029 (2019). https://doi.org/10.1103/PhysRevD.99.044029
[83] A S Lighuda, S D Maharaj, J M Sunzu and E W Mureithi *Astrophys. Space Sci.* **366** 76 (2021). https://doi.org/10.1007/s10509-021-03983-x
[84] L Olengeile, J M Sunzu and J M Mkenyeleye *New Astron.* **100** 102002 (2023). https://doi.org/10.1016/j.newast.2023.102002
[85] J Upreti, S Gedela, N Pant and R P Pant *New Astron.* **80** 101403 (2020). https://doi.org/10.1016/j.newast.2020.101403